



# Mixed-potential-type NO<sub>2</sub> sensor using stabilized zirconia and Cr<sub>2</sub>O<sub>3</sub>–WO<sub>3</sub> nanocomposites

Quan Diao<sup>a</sup>, Chengguo Yin<sup>a</sup>, Yingwei Liu<sup>a</sup>, Jianguo Li<sup>a</sup>, Xun Gong<sup>b</sup>, Xishuang Liang<sup>a,\*</sup>, Shiqi Yang<sup>a</sup>, Hong Chen<sup>b</sup>, Geyu Lu<sup>a,\*\*</sup>

<sup>a</sup> State Key Laboratory on Integrated Optoelectronics, College of Electronic Science and Engineering, Jilin University, 2699 Qianjin Street, Changchun 130012, China

<sup>b</sup> Department of Control Science and Technology, Jilin University, 2699 Qianjin Street, Changchun 130012, China

## ARTICLE INFO

### Article history:

Available online 20 July 2012

### Keywords:

NO<sub>2</sub> sensor

YSZ

Cr<sub>2</sub>WO<sub>6</sub>

Mixed potential

## ABSTRACT

A series of mixed W/Cr oxides with different ratio of W and Cr (1:6, 1:2 and 3:2) have been prepared by using polymeric precursor method. By comparing their sensitivities to 20–300 ppm NO<sub>2</sub>, it was found that the sensor using oxide with 3:2 W/Cr gave the largest response value. For 3:2 W/Cr oxide, the effect of the sintering temperature on the electrode microstructure was also investigated. As a result, the device sintered at 1000 °C showed the best performance. The response value to 100 ppm NO<sub>2</sub> is 51.6 mV, the response time is within 20 s and the sensing device also shows an excellent selectivity against other coexisting gases. The characteristics of SEM and TEM revealed that the special microstructure of oxide electrode formed by sintering plays a significant role in better sensing performance.

© 2012 Elsevier B.V. All rights reserved.

## 1. Introduction

As the increasing of the exhaust emissions from the automotive vehicles and various industrial processes, more and more attentions have been focused on the detection of nitrogen oxides (NO<sub>x</sub>) which give rise to some environmental disaster such as acid rains and photochemical smog. In order to reduce the NO<sub>x</sub> emission from cars, some legislations, such as auto emissions standards of European, America and so on, have been strongly enforced. Therefore, the development of high performance NO<sub>x</sub> sensors is eagerly required [1]. Solid electrolyte gas sensor using yttria stabilized-zirconia (YSZ) and oxide-based sensing electrode (SE) is one of the most advantageous devices, in terms of their special features such as high temperature operation, chemical and mechanical stability, and relatively low fabrication cost [2–13]. In addition, their sensing properties can be tailored by modifying electrode materials.

Up to now, special attentions have been paid to searching for new oxide electrode materials for increasing the sensitivity to NO<sub>2</sub>. The catalytic activity to the reaction of NO<sub>2</sub> decomposition and electrochemical behavior of the SE material are considered to be the main factors to determine the sensitivity [14–19]. The microstructures of the electrodes, such as the particle size, the number of pores and the thickness of the SE layer, considerably affect the

sensitivity and response kinetics of the sensor, because these structural factors can influence the adsorption and desorption on the sensing electrode materials of NO<sub>2</sub> as well as its diffusion in the sensing electrode layer [20,21].

In this work, plenty results of micro-structural and gas sensing characterization of W/Cr binary oxides used as sensing electrodes of mixed-potential NO<sub>2</sub> sensors are presented. We focus on the effect of the ratios and microstructure of W/Cr binary oxides on the sensing properties of the stabilized zirconia-based NO<sub>2</sub> sensors at elevated temperature. The microstructure of W/Cr binary oxides was controlled by the sintering temperature and the doping amount of WO<sub>3</sub> to the oxide electrodes for improving the sensitivity.

## 2. Experimental

### 2.1. Preparation and characterization of the W/Cr binary oxides

The W/Cr binary oxides were prepared with polymeric precursor method, which provides high-dispersion and inhomogeneous mixing W/Cr nanocomposites. In a typical synthesis process, citric acid and stoichiometric amounts of Cr(NO<sub>3</sub>)<sub>3</sub>·9H<sub>2</sub>O and H<sub>40</sub>N<sub>10</sub>O<sub>41</sub>W<sub>12</sub>·xH<sub>2</sub>O were dissolved in deionized water, and molar ratio of citric acid and all the metal cations (Cr and W) was 3:1. Then ethylene glycol was added to the above solution of which the citric acid/ethylene glycol mass proportion was 60%:40%. The resulting solution was maintained at 80 °C to form a polymeric gel, and then calcined at 400 °C for 2 h to remove the polymer, finally sintered at 800 °C for 2 h. We prepared three kinds of W/Cr binary

\* Corresponding author. Tel.: +86 431 85168384; fax: +86 431 85167808.

\*\* Corresponding author. Tel.: +86 431 85167808; fax: +86 431 85167808.

E-mail addresses: [liangxs@jlu.edu.cn](mailto:liangxs@jlu.edu.cn) (X. Liang), [luyg@jlu.edu.cn](mailto:luyg@jlu.edu.cn) (G. Lu).

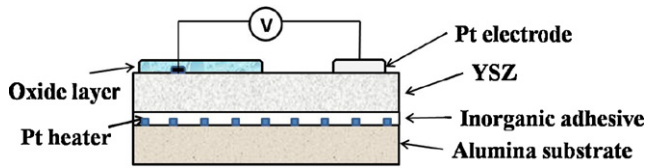


Fig. 1. Schematic cross-sectional view of the planar sensor.

oxides by mixing the W and Cr nitrates with the ratios of 1:6, 1:2 and 3:2. The single  $\text{Cr}_2\text{O}_3$  and  $\text{WO}_3$  were prepared with the same method by using  $\text{Cr}(\text{NO}_3)_3 \cdot 9\text{H}_2\text{O}$  and  $\text{H}_{40}\text{N}_{10}\text{O}_{41}\text{W}_{12} \cdot x\text{H}_2\text{O}$ , respectively.

XRD patterns of the W/Cr binary oxides were measured by Rigaku wide-angle X-ray diffractometer (D/max rA, using  $\text{Cu K}\alpha$  radiation at wavelength  $\lambda = 0.1541 \text{ nm}$ ). Field-emission scanning electron microscopy (FESEM) observations of surface morphology of the sensing electrodes were carried out using a JEOL JSM-7500F microscope with an accelerating voltage of 15 kV. The TEM image was taken by a Philips Tecnai F20 at 200 kV by drop casting the sample dispersions on copper grids.

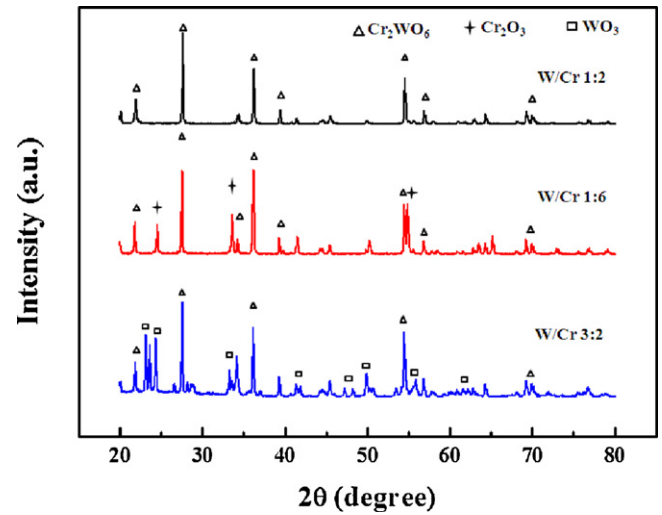


Fig. 2. XRD patterns of W/Cr binary oxides with different ratios sintered at  $800^\circ\text{C}$ .

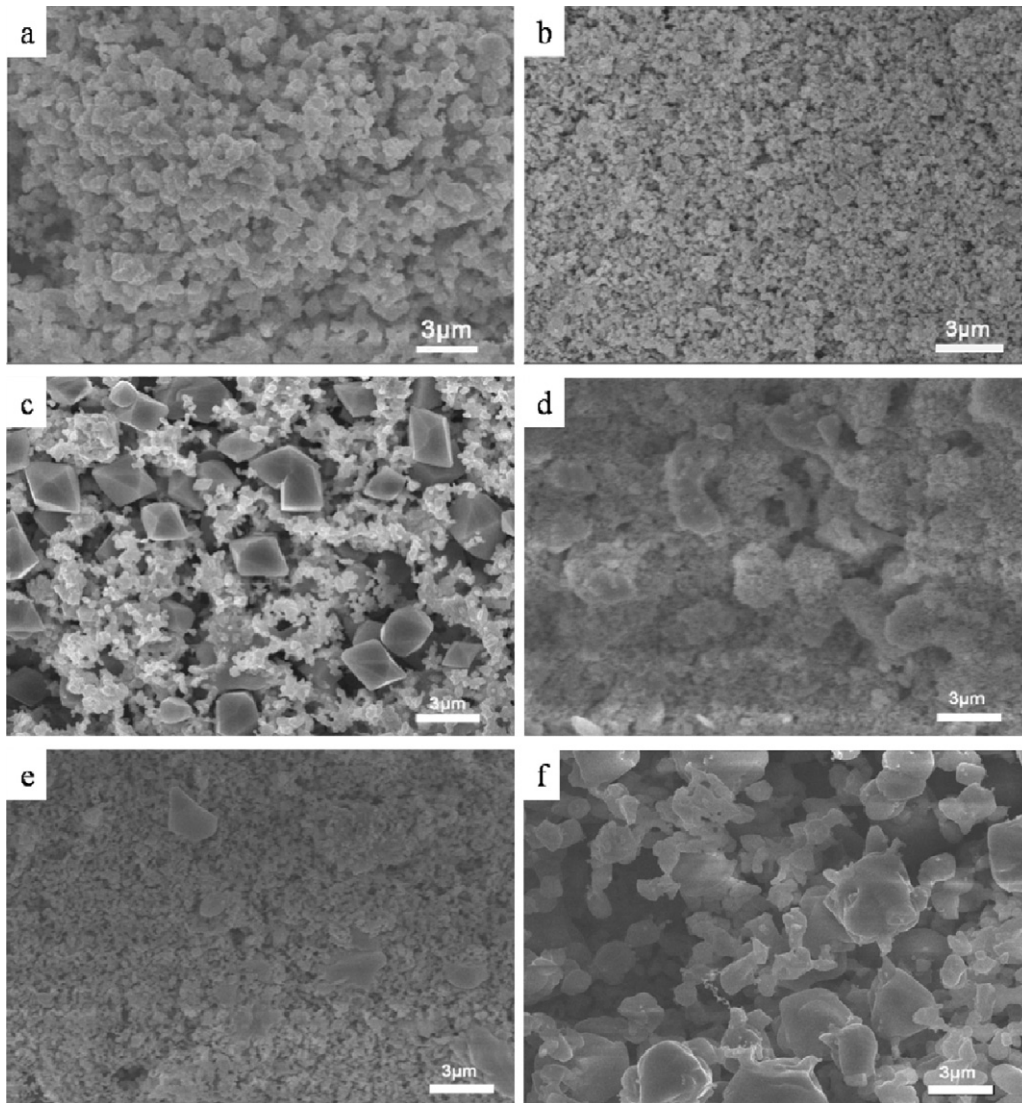


Fig. 3. (i) SEM images of electrode surfaces using W/Cr binary oxides as sensing materials with different ratios: (a) 1:6, (b) 1:2 and (c) 3:2 sintered at  $1000^\circ\text{C}$ ; (ii) electrode surfaces using W/Cr binary oxides with the ratio of 3:2 sintered at different temperatures: (d)  $800^\circ\text{C}$ , (e)  $900^\circ\text{C}$  and (f)  $1100^\circ\text{C}$ .

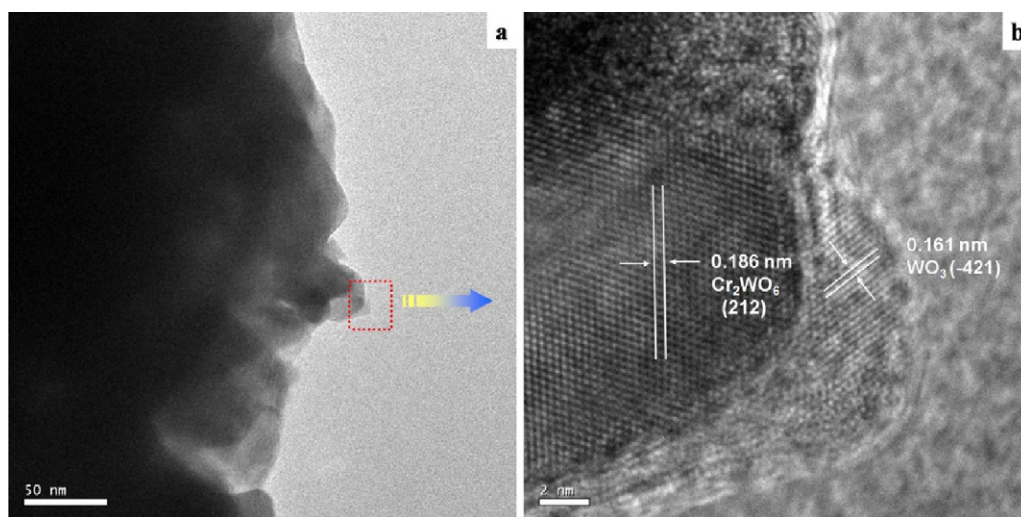


Fig. 4. TEM image (a) and HRTEM image (b) of W/Cr binary oxides with the ratio of 3:2 sintered at 1000 °C.

## 2.2. Fabrication and measurement of the sensor

The sensor was fabricated using YSZ plate (8 mol%  $\text{Y}_2\text{O}_3$ -doped, 2 mm  $\times$  2 mm, 0.2 mm thickness, provided by Tosoh Corp., Japan), as shown in Fig. 1. Two Pt lead wires were attached to the two ends of the YSZ plate with a commercial Pt paste (Sino-platinum Metals CO., Ltd.), and sintered at 800 °C for 2 h. The obtained oxide was mixed with deionized water, fully triturated and the resulting paste was applied on one end of the sensor plate as sensing electrode. Furthermore, to form different surface topography of the sensing electrode material, the device with the 3:2 W/Cr oxide was sintered at 800 °C, 900 °C, 1000 °C and 1100 °C, respectively, and labeled as Sensor A, B, C and D. Then the Pt heater formed on an alumina substrate was attached to the device by using inorganic adhesive, which provides the operating temperature to the sensor.

## 3. Results and discussion

### 3.1. Microstructure characteristics

The XRD patterns of W/Cr binary oxides sintered at 800 °C are shown in Fig. 2. In the figure, the patterns of three W/Cr binary oxides are presented, corresponding to terminal products prepared with different ratios of W and Cr nitrates: 1:6, 1:2 and 3:2. When the ratio is 1:2, the diffraction peaks are in good agreement with the JCPDS (File No. 73-2236) data of  $\text{Cr}_2\text{WO}_6$  tetragonal oxide. When the ratio was changed to 1:6, the pattern contains not only  $\text{Cr}_2\text{WO}_6$ , but also the spectrums of the JCPDS (File No. 84-312) data of  $\text{Cr}_2\text{O}_3$ . On the other hand, when the ratio was adjusted to 3:2, the  $\text{WO}_3$  (File No. 72-1465) can be found besides  $\text{Cr}_2\text{WO}_6$ .

The SEM images of the oxide SEs with different W/Cr ratios sintered at 1000 °C are shown in Fig. 3a–c. Fig. 3a and b exhibits agglomerates of elementary particles, but in Fig. 3c the crystals can be seen clearly. To investigate the influence of the temperature on the electrode, the SEM images of the oxides SEs with the 3:2 W/Cr ratio sintered at 800 °C, 900 °C, and 1100 °C are shown in Fig. 3d–f. In Fig. 3d, it can be seen that the surface of the SE is very rugged, since the solid state reactions hardly take place at 800 °C. When the sintering temperature was raised to 900 °C, the solid state reactions related to  $\text{WO}_3$  and  $\text{Cr}_2\text{WO}_6$  seemed to occur, as a result, some small pores and crystals of  $\text{Cr}_2\text{WO}_6$  started to arise and the surface begins to be flat (Fig. 3e). With the further increasing of the sintering temperature, the  $\text{Cr}_2\text{WO}_6$  crystal becomes larger and  $\text{WO}_3$  partly sublimates, and then the larger  $\text{Cr}_2\text{WO}_6$  crystals are

surrounded by small  $\text{WO}_3$  particles at 1000 °C (Fig. 3c). When the sintering temperature rose to 1100 °C, solid solution of  $\text{Cr}_2\text{WO}_6$  and  $\text{WO}_3$  were formed, and the size of the pore became larger (Fig. 3f). Further information about the electrode microstructure of 3:2 W/Cr binary oxide sintered at 1000 °C was obtained from transmission electron microscope (TEM) (Fig. 4). A local region was selected in the TEM image (Fig. 4a), which is the edge of the crystal. The HRTEM image (Fig. 4b) shows the lattice fringes of the crystal with width of 0.186 nm correspond to the (2 1 2) plane of the  $\text{Cr}_2\text{WO}_6$ , and the lattice fringes of the tiny particles around the crystal with width of 0.161 nm correspond to the (–4 2 1) plane of the  $\text{WO}_3$ . This result clearly indicates the existence of  $\text{Cr}_2\text{WO}_6$  and  $\text{WO}_3$  in the crystals.

### 3.2. Gas sensing properties

Dependence of the  $\Delta\text{EMF}$  on the  $\text{NO}_2$  concentrations for the sensors using W/Cr oxides is shown in Fig. 5. It is seen that the  $\Delta\text{EMFs}$  of all the sensors vary linearly with the logarithm of  $\text{NO}_2$  concentration in the examined range of 20–300 ppm at 800 °C. The sensor using W/Cr ratio of 3:2 shows the largest slope and response value. As a comparison, the sensors using  $\text{Cr}_2\text{O}_3$  and  $\text{WO}_3$  as the sensing electrodes were also fabricated and evaluated. Fig. 6 shows the

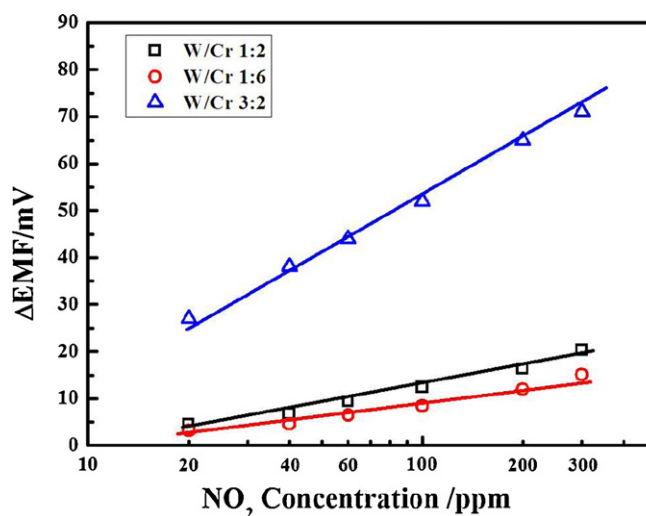


Fig. 5. Dependence of the  $\Delta\text{EMF}$  on the  $\text{NO}_2$  concentrations in the range of 20–300 ppm for sensors using different W/Cr oxides sintered at 1000 °C as SE.



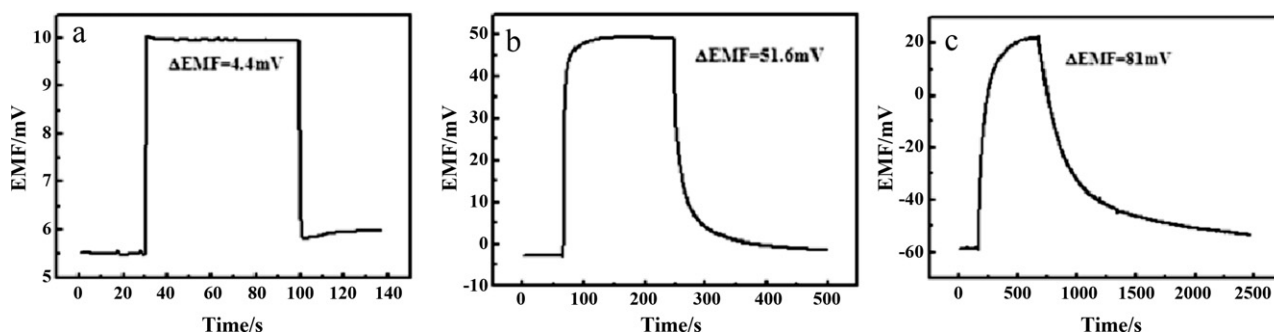


Fig. 6. Response and recovery transients to 100 ppm  $\text{NO}_2$  for the planar sensors attached with (a)  $\text{Cr}_2\text{O}_3$ , (b) 3:2 W/Cr oxide as SE sintered at  $1000^\circ\text{C}$  and (c)  $\text{WO}_3$ .

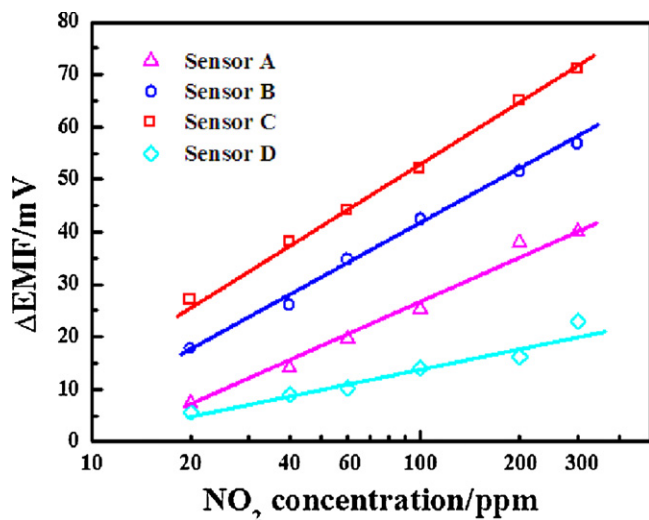


Fig. 7. Dependence of the  $\Delta\text{EMF}$  on the  $\text{NO}_2$  concentrations in the range of 20–300 ppm for the sensors with ratio of 3:2 W/Cr oxide as SE sintered at different temperatures: (A)  $800^\circ\text{C}$ ; (B)  $900^\circ\text{C}$ ; (C)  $1000^\circ\text{C}$  and (D)  $1100^\circ\text{C}$ .

response transients to 100 ppm  $\text{NO}_2$  for the three sensors at  $800^\circ\text{C}$ . It can be observed that the sensor with  $\text{Cr}_2\text{O}_3$  gives the fast response (less than 10 s), but low  $\Delta\text{EMF}$  (about 4.5 mV), the device attached with  $\text{WO}_3$  shows a high  $\Delta\text{EMF}$  (about 80 mV), but its response and recovery are too slow. Comparing with the sensors using the single oxides, the sensor attached with  $\text{Cr}_2\text{WO}_6/\text{WO}_3$  nanocomposite has an acceptable response time (about 20 s) and a  $\Delta\text{EMF}$  value (almost 52 mV). In the case of  $\text{Cr}_2\text{WO}_6/\text{WO}_3$  nanocomposite, the

excellent electrocatalytic activity of  $\text{WO}_3$  seemed to contribute to a high sensitivity to  $\text{NO}_2$ .

In order to investigate the effects of microstructures formed at different sintering temperatures on the sensitivities of the sensors, the four sensors were evaluated at  $800^\circ\text{C}$ . Fig. 7 shows the dependence of  $\Delta\text{EMF}$  on the  $\text{NO}_2$  concentrations for the Sensor A, B, C and D at  $800^\circ\text{C}$ . It is seen that the  $\Delta\text{EMF}$ s of all the sensors are almost linear with the logarithm of  $\text{NO}_2$  concentration in the examined range of 20–300 ppm at  $800^\circ\text{C}$ . Sensor C gives the largest sensitivity (slope) compared with the others, in which the device was sintered at  $1000^\circ\text{C}$ . This can be attributed to the special microstructure of  $\text{Cr}_2\text{WO}_6/\text{WO}_3$  sintered at  $1000^\circ\text{C}$ . As expressed above, the pores accumulated by large particles of  $\text{Cr}_2\text{WO}_6$  and high electrocatalytic activity of  $\text{WO}_3$  to  $\text{NO}_2$  give rise to a high sensitivity to  $\text{NO}_2$  for the Sensor C.

Fig. 8a shows the step-up sensing signal for Sensor C exposed to 2–300 ppm  $\text{NO}_2$  at  $800^\circ\text{C}$ . Both at the low and high concentrations, the response and recovery are fast, and the corresponding dependence of the  $\Delta\text{EMF}$  on concentrations is shown in Fig. 8b. The present device was subjected to additional test, in which, it exposed to 100 ppm  $\text{NO}_2$  repeated 11 times at  $800^\circ\text{C}$ . As shown in Fig. 9, the response transients as well as the potential difference response to 100 ppm  $\text{NO}_2$  are almost reproducible in the successive runs.

The cross-sensitivities to various gases for the Sensor C are exhibited in Fig. 10. It is seen that the present sensor displays rather high selectivity to  $\text{NO}_2$ : the  $\Delta\text{EMF}$  to  $\text{NO}_2$  is more than 50 mV, whereas the  $\Delta\text{EMF}$  values to the other gases are less than 10 mV. Even to 1000 ppm CO and  $\text{CO}_2$ , the Sensor C also gives a rather low response value. It is speculated that in the course of diffusion of the sample gas through the SE layer, the reducing gases (CO,  $\text{CH}_4$  and  $\text{C}_2\text{H}_4$ ) seem to be oxidized to  $\text{CO}_2$  and  $\text{H}_2\text{O}$  due to the pronounced

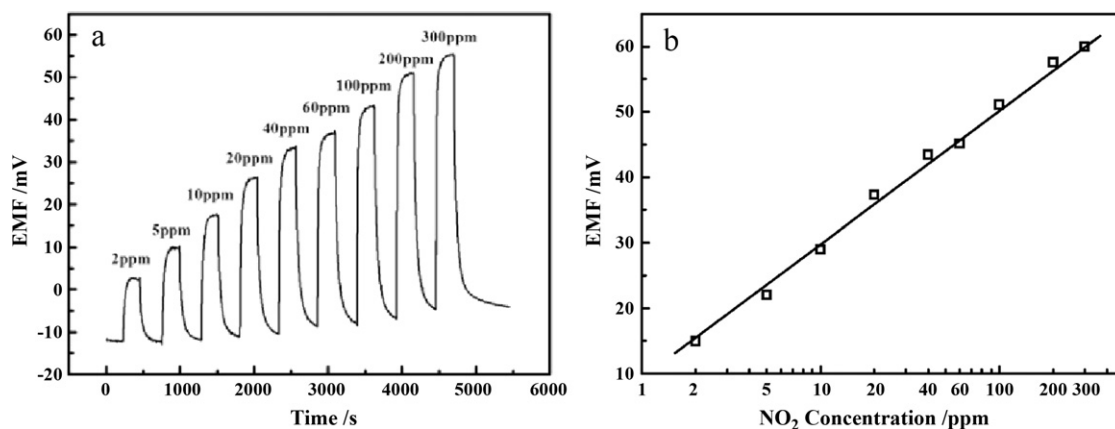


Fig. 8. (a) EMF responses of the sensor with 3:2 W/Cr ratio sintered at  $1000^\circ\text{C}$  to different concentrations of  $\text{NO}_2$  in the range of 2–300 ppm and (b) dependence of the  $\Delta\text{EMF}$  on the logarithm of  $\text{NO}_2$  concentrations at  $800^\circ\text{C}$ .

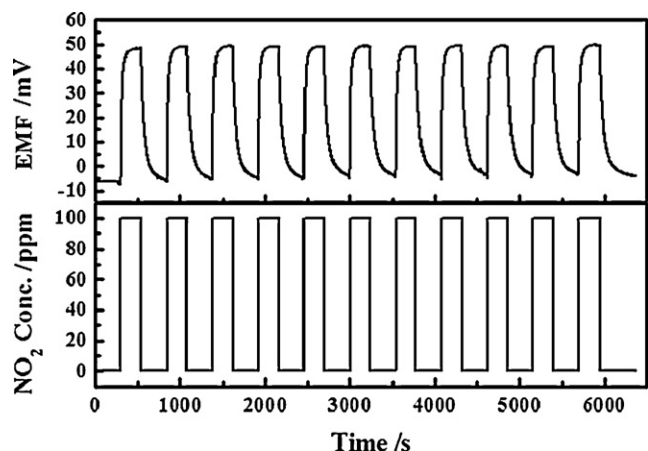


Fig. 9. Repeated response transients of the Sensor C upon switching on- and off- $\text{NO}_2$  at the working temperature of  $800^\circ\text{C}$ .

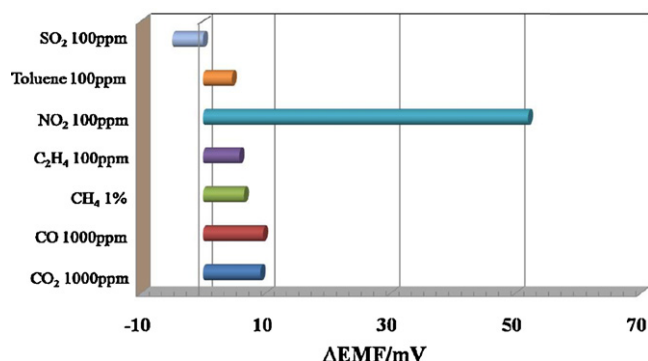


Fig. 10. Cross-sensitivities to various gases for Sensor C at  $800^\circ\text{C}$  with air as balance.

catalytic activity of the  $\text{Cr}_2\text{WO}_6$  at elevated temperature. Also, the response to  $\text{NO}$  was investigated. The response to 200–500 ppm  $\text{NO}$  with air as balance gas is shown in Fig. 11. From the figures, we can see the response value of  $\text{NO}$  is little rather than that of  $\text{NO}_2$ .

Additionally, the influence of the humidity on the sensor was measured, because there is a large amount of water vapor in the car emission exhaust. As shown in Fig. 12, values of the  $\Delta\text{EMF}$  to 100 ppm  $\text{NO}_2$  obtained with different relative humidity (10%, 20%, 50%, 70% and 90%) are less than 5% difference, which shows that the water has little effect on the  $\text{NO}_2$  response for the sensor.

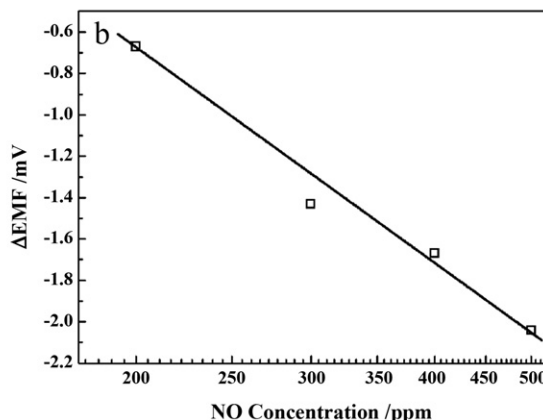
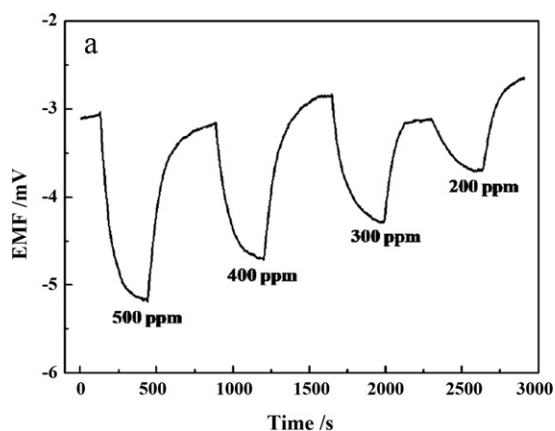


Fig. 11. (a) EMF responses of the sensor with 3:2 W/Cr ratio sintered at  $1000^\circ\text{C}$  to different concentrations of  $\text{NO}$  in the range of 200–500 ppm and (b) dependence of the  $\Delta\text{EMF}$  on the logarithm of  $\text{NO}$  concentrations.

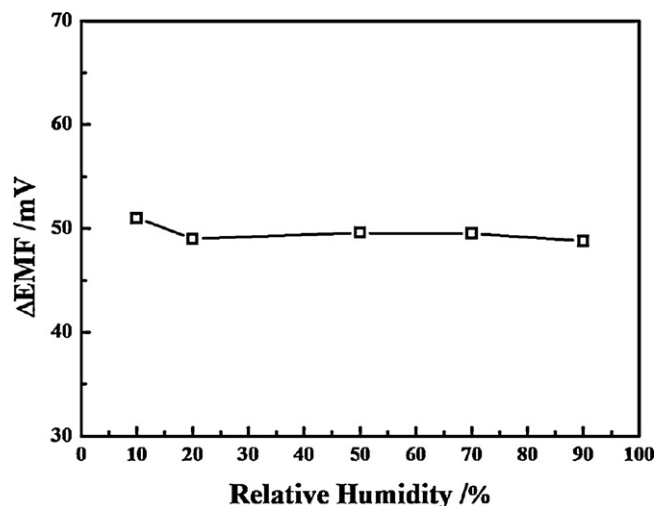
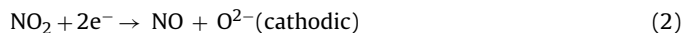
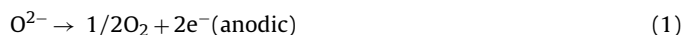


Fig. 12. Response of Sensor C to 100 ppm  $\text{NO}_2$  under different humid atmosphere.

The sensing behavior of the potentiometric  $\text{NO}_2$  sensor has been explained by the mixed potential mechanism [9,22]. When the SE is exposed to  $\text{NO}_2$  in  $\text{O}_2$ -containing atmosphere, a non-Nernstian potential is produced on the SE, because two electrochemical reactions take place at same time on the SE:



Here, the decomposition reaction related to  $\text{NO}_2$  should be mentioned, since it also affects the sensitivity of the sensor.



The reaction (3) is an adverse reaction to the sensitivity of the sensor. When the gas diffuses through the sensing electrode layer, the reaction (3) reduces the  $\text{NO}_2$  concentration and results in a low sensitivity. Since the oxide electrode always has the catalytic activity to the  $\text{NO}_2$  decomposition more or less and the porous microstructure of the electrode is usually utilized to enhance the diffusion of the  $\text{NO}_2$  in the sensing electrode layer as to reduce the consumption of the  $\text{NO}_2$  concentration. For the Sensor C, the larger particle size of  $\text{Cr}_2\text{WO}_6$  enhances the porosity of the nanocomposite oxide and promotes the diffusion of  $\text{NO}_2$  in oxide layer. At same time, the outstanding electrocatalytic activity of  $\text{WO}_3$  to reaction (2) raises the  $\Delta\text{EMF}$  to  $\text{NO}_2$ . The above two parameters jointly determined the good sensing performance of the sensor using 3:2 W/Cr oxides.

#### 4. Conclusions

The W/Cr binary oxides SE layers with different ratios were formed on the YSZ plate. It is found that the sensor using W/Cr binary oxides with the ratio of 3:2 has the optimal NO<sub>x</sub> sensing characteristic. Moreover, the sensors sintered at various temperatures (800 °C, 900 °C, 1000 °C and 1100 °C) were prepared and tested. The results revealed that the sensor sintered at 1000 °C exhibits the highest sensitivity and speedy response and recovery rates. The high sensitivity and the fast response rate can be attributable to its special porous microstructure, which results from the sublimation of the WO<sub>3</sub>, the growth of the Cr<sub>2</sub>WO<sub>6</sub> particles as well as the synergy of the WO<sub>3</sub> and Cr<sub>2</sub>WO<sub>6</sub>. In addition, the sensor has a rather good selectivity to NO<sub>2</sub>. These good sensing properties indicate the promising potential of the sensor in practical application.

#### Acknowledgement

Supported by NSFC (No. 61074172) (No. 61134010) (No. 61104203) and Program for Chang Jiang Scholars and Innovative Research Team in University (No. IRT1017), and Jilin province science and technology development plan program (20106002) is gratefully acknowledged.

#### References

- [1] N. Docquier, S. Candel, Combustion control and sensors: a review, *Progress in Energy and Combustion Science* 28 (2002) 107–150.
- [2] N. Miura, G. Lu, N. Yamazoe, H. Kurosawa, M. Hasei, Mixed potential type NO<sub>x</sub> sensor based on stabilized zirconia and oxide electrode, *Journal of the Electrochemical Society* 143 (1996) L33–L35.
- [3] N. Miura, H. Kurosawa, M. Hasei, G. Lu, N. Yamazoe, Stabilized zirconia-based sensor using oxide electrode for detection of NO<sub>x</sub> in high-temperature combustion-exhausts, *Solid State Ionics* 86–88 (1996) 1069–1073.
- [4] T. Hibino, K. Ushiki, Y. Kuwahara, Electrochemical oxygen pump using CeO<sub>2</sub>-based solid electrolyte for NO<sub>x</sub> detection independent of O<sub>2</sub> concentration, *Solid State Ionics* 93 (1997) 309–314.
- [5] E.L. Broscha, R. Mukundan, D.R. Brown, F.H. Garzon, Mixed potential sensors using lanthanum manganate and terbium yttrium zirconium oxide electrodes, *Sensors & Actuators B: Chemical* 87 (2002) 47–57.
- [6] N.F. Szabo, P.K. Dutta, Correlation of sensing behavior of mixed potential sensors with chemical and electrochemical properties of electrodes, *Solid State Ionics* 171 (2004) 183–190.
- [7] U. Guth, J. Zosel, Electrochemical solid electrolyte gas sensors—hydrocarbon and NO<sub>x</sub> analysis in exhaust gases, *Ionics* 10 (2004) 366–377.
- [8] N. Miura, J. Wang, M. Nakatou, P. Elumalai, M. Hasei, NO<sub>x</sub> sensing characteristics of mixed-potential-type zirconia sensor using NiO sensing electrode at high temperatures, *Electrochemical and Solid-State Letters* 8 (2005) H9–H11.
- [9] P. Elumalai, J. Wang, S. Zhuikov, D. Terada, M. Hasei, N. Miura, Sensing characteristics of YSZ-based mixed-potential-type planar NO<sub>x</sub> sensors using NiO sensing electrodes sintered at different temperatures, *Journal of the Electrochemical Society* 152 (2005) H95–H101.
- [10] P. Elumalai, V.V. Plashnitsa, T. Ueda, M. Hasei, N. Miura, Dependence of NO<sub>2</sub> sensitivity on thickness of oxide-sensing electrodes for mixed-potential-type sensor using stabilized zirconia, *Ionics* 12 (2006) 331–337.
- [11] J.W. Fergus, Materials for high temperature electrochemical NO<sub>x</sub> gas sensors, *Sensors & Actuators B: Chemical* 121 (2006) 652.
- [12] J. Gao, J. Viricelle, C. Pijolat, P. Breuil, P. Vernoux, A. Boreave, A. Giroir-Fendler, Improvement of the NO<sub>x</sub> selectivity for a planar YSZ sensor, *Sensors & Actuators B: Chemical* 154 (2011) 106–110.
- [13] X.S. Liang, S.Q. Yang, J.G. Li, H. Zhang, Q. Diao, W. Zhao, G. Lu, Mixed-potential-type zirconia-based NO<sub>2</sub> sensor with high-performance three-phase boundary, *Sensors & Actuators B: Chemical* 158 (2011) 1–8.
- [14] J. Yoo, E.D. Wachsman, NO<sub>2</sub>/NO response of Cr<sub>2</sub>O<sub>3</sub>- and SnO<sub>2</sub>-based potentiometric sensors and temperature-programmed reaction evaluation of the sensor elements, *Sensors & Actuators B: Chemical* 123 (2007) 915–921.
- [15] J. Park, B.Y. Yooh, C.O. Park, W. Lee, C.B. Lee, Sensing behavior and mechanism of mixed potential NO<sub>x</sub> sensors using NiO, NiO(+YSZ) and CuO oxide electrodes, *Sensors & Actuators B: Chemical* 135 (2009) 516–523.
- [16] N. Miura, J. Wang, P. Elumalai, T. Ueda, D. Terada, M. Hasei, Improving NO<sub>2</sub> sensitivity by adding WO<sub>3</sub> during processing of NiO sensing-electrode of mixed-potential-type zirconia-based sensor, *Journal of the Electrochemical Society* 154 (2007) J246–J252.
- [17] P. Elumalai, N. Miura, Performances of planar NO<sub>2</sub> sensor using stabilized zirconia and NiO sensing electrode at high temperature, *Solid State Ionics* 176 (2005) 2517–2522.
- [18] V.V. Plashnitsa, T. Ueda, P. Elumalai, T. Kawaguchi, N. Miura, Zirconia-based planar NO<sub>2</sub> sensor using ultrathin NiO or laminated NiO–Au sensing electrode, *Ionics* 14 (2008) 15–25.
- [19] G. Lu, N. Miura, N. Yamazoe, Stabilized zirconia-based sensors using WO<sub>3</sub> electrode for detection of NO or NO<sub>2</sub>, *Sensors & Actuators B: Chemical* 65 (2000) 125–127.
- [20] L.P. Martin, A.Q. Pham, R.S. Glass, Effect of Cr<sub>2</sub>O<sub>3</sub> electrode morphology on the nitric oxide response of a stabilized zirconia sensor, *Sensors & Actuators B: Chemical* 96 (2003) 53–60.
- [21] B. White, S. Chatterjee, E. Macam, E. Wachsman, Effect of electrode microstructure on the sensitivity and response time of potentiometric NO<sub>x</sub> sensors, *Journal of the American Ceramic Society* 91 (2008) 2024–2031.
- [22] N. Miura, H. Kuroaswa, M. Hasei, G. Lu, N. Yamazoe, Stabilized zirconia-based sensor using oxide electrode for detection of NO<sub>x</sub> in high-temperature combustion-exhausts, *Solid State Ionics* 86–87 (1996) 1069–1073.

#### Biographies

**Diao Quan** received the bachelor degree in Department of Chemistry in 2008. He is currently studying for his Dr. Sci. degree in College of Electronic Science and Engineering, Jilin University, China.

**Yin Chengguo** received the B.Eng. degree in Department of Electronic Sciences and Technology in 2010. He is currently studying for his M.E. Sci. degree in College of Electronic Science and Engineering, Jilin University, China.

**Liu Yingwei** received the B.Eng. degree in Department of Electronic Sciences and Technology in 2010. He is currently studying for his M.E. Sci. degree in College of Electronic Science and Engineering, Jilin University, China.

**Li Jianguo** received the B.Eng. degree in Department of Electronic Sciences and Technology in 2010. He is currently studying for his M.E. Sci. degree in College of Electronic Science and Engineering, Jilin University, China.

**Gong Xun** received the bachelor degree in Department of Electrical Engineering and Automation from the Northeast Electrical University in 2006, China. He is a student with successive postgraduate and doctoral programs of study at the Jilin University, China. His current research interests are in the development of engine electronic control and the application of the engine sensors.

**Liang Xishuang** received the B.Eng. degree in Department of Electronic Sciences and Technology in 2004. He received his Doctor's degree in College of Electronic Science and Engineering at Jilin University in 2009. Now he is a lecturer of Jilin University, China. His current research is solid electrolyte gas sensor.

**Yang Shiqi** received the B.Eng. degree in Department of Electronic Sciences and Technology in 2009. He is currently studying for his M.E. Sci. degree in College of Electronic Science and Engineering, Jilin University, China.

**Chen Hong** received the B.S. and M.S. degrees in process control from Zhejiang University, Hangzhou, China, in 1983 and 1986 respectively, and the Ph.D. degree from the University of Stuttgart, Stuttgart, Germany, in 1997. Since 1999, she has been a professor at the Jilin University. Her current research interests include model predictive control, optimal and robust control, and applications in mechatronic systems.

**Lu Geyu** received the B. Sci. degree in electronic sciences in 1985 and the M. Sci. degree in 1988 from Jilin University in China and the Dr. Eng. degree in 1998 from Kyushu University in Japan. Now he is a professor of Jilin University, China. His current research interests include the development of chemical sensors and the application of the function materials.